Grenze International Journal of Engineering and Technology, June Issue

Behavior of Industrial Chimneys Subjected to Dynamic Loading using ANSYS: A Parametric and Modal Response-based Approach

Kuntal Zade[1] and Sanket Sanghai[2]
[1-2]Department of Civil Engineering, G H Raisoni College of Engineering, Nagpur, MH, India
Email: kuntalzade@gmail.com, sanket.sanghai@raisoni.net

***Abstract*— The industrial chimneys exist as slender reinforced concrete towers which must resist the wind forces, seismic activity, as well as sudden dynamic loads. The current design methods rely on simplified static approaches, or the equivalent dynamic procedures which lead to conservative designs that do not represent the actual structural response under the time-based loading conditions. The increasing height as well as flexibility of the industrial chimneys require the development of design procedures which directly evaluate the dynamic behavior as well as the material performance efficiency. The study develops the industrial chimney optimization framework which uses the ANSYS for the finite element-based analysis which applies the Genetic Algorithm to optimize the dynamic performance under the actual loading conditions. The researchers created the explicit model which includes the gravity forces, height dependent wind pressure, seismic time history excitation as well as the short duration gust impulses to achieve physical accuracy and reproducibility. The numerical results show that the optimized chimney achieved 18% reduction in the structural mass, 22.5 % reduction in the peak base stress, as well as 32 % decrease in the harmonic displacement when compared with the baseline design. Fundamental natural frequency increased from 0.82 Hz to 0.93 Hz which reduced the resonance susceptibility. The seismic time history analysis showed reduced base moments as well as the smoother displacement response which resulted from the improved stiffness distribution as well as damping effects. The key innovation of this research combines the transient loading assessment with the complete response evaluation as well as geometric optimization within one ANSYS based system which supports the industrial chimney structures that remain sensitive to the dynamic forces.**

***Index Terms*— ANSYS, design optimization, dynamic loading, industrial chimney, finite element analysis (FEA), genetic algorithm.**

I. INTRODUCTION

Industrial chimneys provide the essential vertical components which handle flue gas, and particulate matter emissions from the industrial processes as well as manufacturing operations, and the power generation activities to permit safe atmospheric discharge. Their function ensures the environmental compliance as well as operational safety [1]. Industrial capacity expansion has driven chimney design changes which require the taller, and thinner structures to enhance the dispersion efficiency while managing the higher temperature exhaust emissions.

Grenze ID: 01.GIJET.12.2.397_22

Wind gusts as well as vortex shedding, and seismic excitations create the increased dynamic actions which these configurations face as the inherent problem. The combination of the reduced mass as well as high flexibility, and the slender geometry create design challenges which require solutions to manage the lateral displacements as well as cyclic stresses, and the potential resonance problems [2,3].

Historical evidence shows that many chimney failures are governed by the dynamic effects because the structures lack sufficient static strength. Wind-induced vibrations initiate fatigue cracking when they reach the base, or openings of the reinforced concrete chimneys while seismic excitation produces severe damage through the structural frequency alignment with the ground motion patterns [4][5]. The current practice of the chimney design requires engineers to perform the precise dynamic response assessment together with its corresponding mitigation methods. Current design approaches rely largely on the deterministic code provisions which simplify loading conditions as well as neglect how geometric parameters affect the dynamic behavior. The modal properties of the system show significant changes based on the following three factors which include the taper ratio as well as wall thickness distribution, and the material stiffness. The limitation leads to two outcomes which include the conservative designs that require excessive material usage, and costs, or the unsafe situations that allow resonance as well as fatigue risks to continue. Existing research primarily addresses the static, or modal analysis independently with the limited integration of the advanced optimization strategies [6][7]. The research gaps exist because the essential design elements that affect the frequency response as well as dynamic amplification remain unstudied according to the existing studies.

The research establishes, and validates the optimization framework which operates through the finite element analysis to assess the dynamic performance of the reinforced concrete chimneys. The methodology uses ANSYS Workbench to combine its three analysis types with the metaheuristic optimization technique which evaluates the design parameters. The objective is to achieve the reduced structural weight while ensuring the dynamic stability [8,9]. The proposed framework enables the systematic exploration of the design alternatives as well as demonstrates the improved performance compared to the conventional methods, which lead to safer as well as more efficient chimney structures.

II. METHODOLOGY

A. Model Geometry

The reference geometry corresponds to the cooling tower that is made of reinforced concrete as well as the tapered which is the common type used in thermal, and the process industries. The principal geometric parameters are disclosed in Table 1. The structure exists as the vertical cantilever that has its foundation point fixed while its chimney base connects to the solid pedestal.

TABLE I: BASELINE GEOMETRIC AND MATERIAL PARAMETERS OF THE CHIMNEY MODEL

Parameter	Symbol	Value / Range	Unit	Description
Height	H	80	m	Overall height of chimney
Base diameter	D_{base}	8.0	m	Diameter at bottom section
Top diameter	D_{top}	4.0	m	Diameter at outlet
Wall thickness	t	0.30–0.50	m	Varies with optimization
Material grade	$M40$	–	–	Reinforced concrete grade
Elastic modulus	E	34 × 10^9	Pa	Tangent modulus for concrete
Density	ρ	2500	kg/m³	Self-weight and inertia loading
Poisson's ratio	ν	0.20	–	Lateral strain relation
Damping ratio	ξ	0.05	–	Structural damping for dynamic response

B. Loading Conditions and Load Combinations

In the present study, all loading conditions were explicitly defined and applied in accordance with Indian Standard provisions to ensure realism, reproducibility, and compliance with codal requirements. The loads were categorized into gravity loads, wind-induced loads, seismic excitation, and transient gust effects. Each load type was applied independently as well as in relevant combinations for static and dynamic analyses.

C. Gravity Loads

Gravity loads represent permanent actions acting on the chimney during its service life, including the self-weight of the reinforced concrete shell and the internal lining and insulation. The self-weight was computed automatically in ANSYS using a concrete density of 25 kN/m³ and gravitational acceleration of 9.81 m/s² applied as a global setting. In addition, a uniform internal surface pressure of 3 kN/m² was assigned to simulate refractory lining and insulation.

D. Wind Loading

The evaluation of wind loading was conducted according to IS 875 (Part 3) standards from 2015 which required assessment of wind pressure variations that depend on chimney height. The structure's slender design required engineers to treat wind effects as the main dynamic force that affected its movement. The design wind speed at height z was calculated using [12]:

$$V_z = V_b\, k_1\, k_2\, k_3 \quad (2)$$

Where, V_b denotes as the basic wind speed, k_1 as the risk coefficient, k_2 as the terrain, height, and the structure size factor, and k_3 denotes as the topography factor. The corresponding wind pressure was computed as the following:

$$p_z = 0.6\, V_z^2$$

The wind pressure was applied as the circumferentially distributed surface pressure on the chimney shell which created the vertical pressure distribution that increased with the height.

E. Seismic Loading

The seismic loading was determined as based on IS 1893 (Part 1): 2016 which has treated the chimney as the vertical cantilevered concrete structure that had its base fixed. The design horizontal seismic coefficient was calculated using [13]:

$$A_h = \frac{Z}{2} \cdot \frac{I}{R} \cdot \frac{S_a}{g} \quad (2)$$

here Z is the seismic zone factor, I the importance factor, R is the response reduction factor, and S_a/g is the spectral acceleration coefficient

The El Centro (1940) earthquake record was scaled to match the target PGA, and applied as the horizontal base acceleration in the time-history analysis.

F. Load Combinations

To represent realistic operating conditions, appropriate load combinations were defined for each analysis stage in accordance with standard engineering practice and code recommendations. Static analysis considered gravity with wind loading, while modal analysis included gravity effects only. Harmonic response was evaluated under combined gravity and harmonic wind excitation. Transient analysis incorporated gravity with a wind gust impulse, and seismic assessment used gravity with base excitation. Each case was applied separately to clearly identify its influence, followed by a comparative assessment of structural response.

G. Transient Gust Loading Definition and Implementation

Mathematical Formulation of Gust Impulse

The gust load was represented using the sinusoidal pulse function which produced the smooth pressure onset, and decay while the function accurately simulated the sudden pressure changes that occur during the wind gusts. The pressure variation with the time was defined as [14]:

$$p(t) = \begin{cases} p_{\max} \sin\left(\frac{\pi t}{T_g}\right), & 0 \le t \le T_g \\ 0, & t > T_g \end{cases} \quad (3)$$

here $p(t)$ is the transient wind pressure at time t, $p_{\max}$ is the peak gust pressure amplitude, and T_g is the gust duration

The formula establishes the pressure conditions which remain nonexistent at both the beginning, and the conclusion of the gust event, thus preventing numerical discontinuities during the analysis of the transient response.

H. Gust Load Parameters

The gust impulse parameters were selected based on standard extreme wind data for tall slender structures and aligned with code-based wind pressure provisions. A peak gust pressure amplitude of 2.5 kPa was adopted to

represent a temporary increase beyond the mean design wind load, applied over a duration of 3 s using a sinusoidal pulse function. The wind direction served as the path for the load application which researchers studied through the transient dynamic analysis.
The selected method provides the authentic representation of the short-term extreme gust impacts which determine how these structures respond.

I. Implementation of Gust Load in ANSYS

The researchers conducted their study by using ANSYS for simulating the transient gust loading through the implementation of the time-dependent surface pressure during their transient structural analysis work [10,11]. The researchers applied the load to shell elements throughout the entire defined height by implementing the pressure-time function which they obtained from the sinusoidal pulse [12,13]. The gust event started at the beginning of 3.0 second load step which continued with the 7.0 seconds of free vibration to observe the decay behavior resulting in the overall analysis duration of 10.0 seconds. The time step of 0.01 seconds enabled the system to achieve the sufficient response measurement precision. The researchers used 5% Rayleigh damping ratio to model the structural damping which enabled them to accurately depict the energy dissipation during loading as well as subsequent periods.

III. Results and Discussion

A. Comparison of Chimney Configuration Before and After Optimization

The optimization needs assessment through the physical design changes which proved successful in the methodology.

B. Geometric Modifications Induced by Optimization

The optimization revised wall thickness distribution and taper ratio under stress, displacement, and frequency constraints.
Unlike the conventional uniform design with excess base mass, the optimized model allocates material more efficiently along the height, reducing base thickness while maintaining stiffness through an improved taper configuration (see Table 2).

TABLE II: KEY GEOMETRIC PARAMETERS COMPARISON OF BEFORE AND AFTER OPTIMIZATION

Parameter	Baseline Design	Optimized Design	Change
Base wall thickness (m)	0.45	0.38	↓ 15%
Top wall thickness (m)	0.30	0.28	↓ 7%
Base diameter (m)	8.0	8.0	No change
Top diameter (m)	4.0	4.3	↑ 7.5%
Taper ratio (D_{base}, D_{top})	2.0	1.86	Optimized
Slenderness ratio (H/D_{top})	20.0	18.6	↓ 7%

The study found that reducing the taper ratio brought better lateral stiffness results together with the better dynamic stability performance because there was no added weight to the system.

C. Structural Mass and Stiffness Redistribution

The optimization process aimed to achieve two main goals which required the team to reduce the total structural weight while maintaining the existing dynamic performance [14,15]. The optimized design achieved the significant reduction in the mass through controlled material redistribution which the designers used instead of applying the uniform thinning (see Table 2).

TABLE III: STRUCTURAL MASS AND STIFFNESS-RELATED COMPARISON

Parameter	Baseline Design	Optimized Design	Improvement
Total structural mass (kg)	1.62×10^6	1.32×10^6	↓ 18%
Mass per unit height (average) (kg/m)	20,250	16,500	↓ 18.5%
Flexural rigidity near base (EI)	Reference	↑ Increased	Improved
Mass eccentricity	Higher	Reduced	Improved

With optimization of the mass distribution, the inertial forces were reduced under the dynamically loading condition, which is leading to the lower basic moments, and low stress demand.

D. Effect of Optimization on Dynamic Stiffness and Natural Frequency

The chimney's dynamic properties changed due to the project changed its mass, and stiffness distribution. The fundamental natural frequency of the system increased which shows that the system gained better resistance to the wind-induced resonance given in Table 3.

TABLE IV: DYNAMIC PERFORMANCE COMPARISON BEFORE AND AFTER OPTIMIZATION

Dynamic Parameter	Baseline	Optimized	Change
First natural frequency (Hz)	0.82	0.93	↑ 13.4%
Frequency separation from wind band	Marginal	Adequate	Improved
Peak harmonic displacement (mm)	28.6	19.4	↓ 32%
Dynamic amplification factor	1.82	1.48	↓ 18.6%

The structure's natural frequency increase moved it beyond the critical wind excitation range which led to decreased the resonance susceptibility as well as lower vibration amplitude.

E. Quantitative Link Between Design Changes and Performance Gains

Design changes which the optimization brought to the system created performance improvements. The building design used thinner walls which is reduced the construction weight as well as seismic resistance while making the design more stable through the better tapering.

The system achieved better vibration control, and lower stress points through these modifications which resulted in the increased durability.

The structure reached better dynamic performance through the safety as well as serviceability requirements which it successfully fulfilled.

F. Dynamic Response Evaluation Parameters

The natural frequency is used as the primary method which engineers the use to evaluate how the tall chimneys react to resonance, although this method fails to provide the complete information about their structural performance in the dynamic loading tests.

The research study used six measurement variables which included the displacement response as well as the base shear to conduct its post-analysis assessment.

The safety assessment used these parameters to determine the serviceability, and dynamic stability during the wind as well as the seismic events.

G. Peak Displacement Response

The maximum lateral displacement for the slender structures which include the industrial chimneys serves as the critical serviceability standard because the excessive movement results in structural damage through the cracking as well as material loss which eventually leads to the durability problems. The peak displacement at the top of structure occurred during the static wind conditions, and through the application of harmonic as well as seismic loads which are detailed in Table 4.

The optimized design showed the decreased peak responses because it achieved better stiffness distribution, and also it minimized the total inertial mass.

TABLE V: COMPARISON OF PEAK DISPLACEMENT RESPONSE

Load Case	Baseline Design	Optimized Design	Reduction
Static wind (mm)	21.3	15.8	↓ 25.8%
Harmonic excitation (mm)	28.6	19.4	↓ 32.2%
Seismic time-history (mm)	67.0	54.6	↓ 18.5%

Showing that however the small reductions in displacement, improved geometry allows for the larger increase in the optional geometric controllability without the increased energy content requirements.

H. Stress Demand and Distribution

The structural safety, and durability of the building system depend on the stress demand which reaches its peak at the base when bending moments become the most intense. The maximum compressive stresses were determined by assessing the shell elements located on the leeward side. The optimized configuration achieved the uniform stress distribution because it decreased the peak stress values through its improved taper efficiency which resulted in the lower mass concentration, as shown in Table 5.

TABLE VI: MAXIMUM STRESS COMPARISON AT CHIMNEY BASE

Parameter	Baseline	Optimized	Improvement
Peak compressive stress (MPa)	18.2	14.1	↓ 22.5%
Stress utilization ratio	0.76	0.59	Improved
Stress concentration	Localized	Distributed	Improved

The evaluation results showed that stress values remained below the maximum limits in which IS 6533 established as well as showed that the structure maintained its operational capacity.

I. Base Shear and Base Moment Response

The base shear as well as base moment measurements demonstrate how the structural demands transfer to the foundation which serves as the primary determinant of structural stability during the dynamic events. The chimney design received the optimization because its reduced mass, as well as the better stiffness distribution led to decreased the base reaction forces (see Table 6).

TABLE VII: COMPARISON OF BASE SHEAR AND BASE MOMENT

Parameter	Baseline	Optimized	Reduction
Peak base shear (kN)	1,180	960	↓ 18.6%
Peak base moment ($N \cdot m$)	4.20×10^6	3.42×10^6	↓ 18.6%

This reduction of special notice for the foundation engineering, and the footing behavior under repeating the dynamic loading events in the longer-term context.

J. Dynamic Amplification Factor (DAF)

The Dynamic Amplification Factor was calculated as the ratio of maximum dynamic displacement to corresponding the static displacement given in Table 7. The DAF value functions as the essential measurement which determines the vibration response sensitivity during the dynamic tests [19][20].

TABLE VIII: DYNAMIC AMPLIFICATION FACTOR COMPARISON

Design	Static Displacement (mm)	Dynamic Displacement (mm)	DAF
Baseline	21.3	38.8	1.82
Optimized	15.8	23.4	1.48

The reduction in the DAF demonstrates that the optimized design effectively mitigates resonance, and the vibration amplification.

K. Comprehensive Performance Comparison

Key response parameters are provided so as to offer the all-embracing structural performance given in Table 8.

TABLE IX: COMPREHENSIVE DYNAMIC PERFORMANCE COMPARISON

Performance Metric	Baseline	Optimized	Improvement
First natural frequency (Hz)	0.82	0.93	↑ 13.4%
Peak top displacement (mm)	67.0	54.6	↓ 18.5%
Peak base stress (MPa)	18.2	14.1	↓ 22.5%
Base shear (kN)	1,180	960	↓ 18.6%
Base moment (N·m)	4.20×10^6	3.42×10^6	↓ 18.6%
Dynamic amplification factor	1.82	1.48	↓ 18.6%

L. Modal Analysis

The modal analysis was conducted on both the baseline, as well as optimized configurations revealed the natural frequencies, and their corresponding deformation shapes. The first three modes which showed the significance to the study occurred within frequency range that given in Table 9 which shows for both the wind as well as seismic excitations.

TABLE X: MODAL CHARACTERISTICS OF CHIMNEY STRUCTURE

Mode	Frequency (Hz)	Description	Comment
1	0.82	1st bending (SW direction)	Dominant mode
2	0.85	1st bending (NW direction)	Orthogonal
3	2.41	1st torsional	Negligible participation

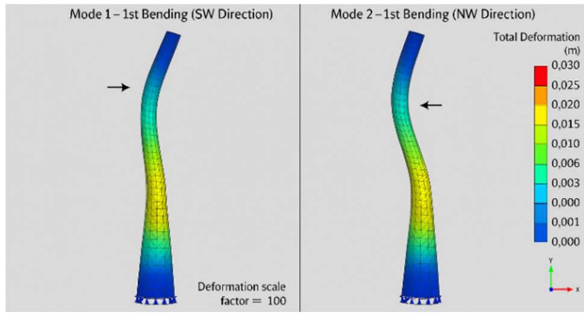

Fig. 1. The first (bending) as well as second (orthogonal) vibration patterns obtained from the ANSYS modal analysis

The base configuration shows the first bending frequency of 0.82 Hz which is shown in Fig. 1, which lies within the typical wind excitation range of 0.7 to 1.0 Hz for the tall chimneys thus indicating the possible resonance under the strong wind conditions. The optimization process led to the increased structural stiffness which resulted in the upward shift of natural frequency that reached 13.4% increase because it moved beyond the critical range. The parametric analysis shows that 20% increase in the wall thickness results in the fundamental frequency increase of approximately 15% because mass as well as stiffness factors control the frequency response. The additional thickness results in the increased self-weight as well as base moment which requires designers to find the appropriate balance between both the design elements. The first two bending modes demonstrate how structures respond to the dynamic loading through their ability to bend by sideways.

M. Processing of Seismic Input and Interpretation of Time-History Response

Physical Explanation for the Smooth Displacement Response

The earthquake record shows the non-stationary behavior with irregular frequency content, whereas the top displacement response appears smooth. The response functions through the first-mode control which governs the slender cantilever system while the mass-stiffness characteristics filter out the high-frequency elements. The 5 damping ratio decreases the rapid oscillations which occur during the response. The shell shape enables the gradual distribution of forces throughout the structure. The smooth displacement response shows the actual structural behavior because it exists as the real physical movement instead of the numerical computation error.

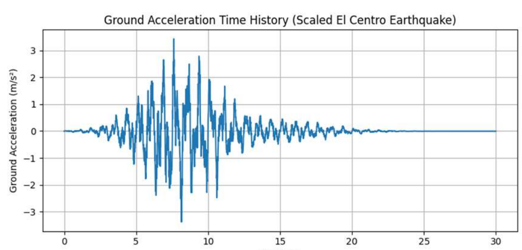

Fig. 2. Ground acceleration time history of the scaled El Centro earthquake.

The seismic input used in the study was derived from the El Centro acceleration record which appeared in Fig 2 after study conducted the baseline correction as well as scaling procedures. The record demonstrates the non-stationary behavior through its changing intensity levels, as well as its evolving sound frequencies.

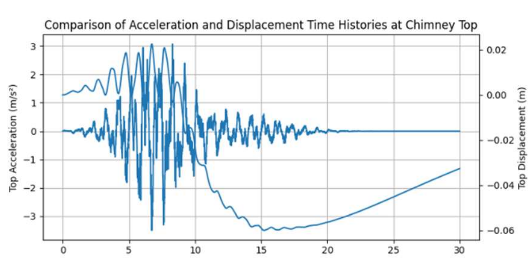

Fig. 3. Comparison of the acceleration as well as displacement time histories at the top of chimney.

The results show that at the top of chimney, both the acceleration as well as displacement responses showed the particular patterns which developed throughout the testing process.

IV. CONCLUSIONS

This research develops the optimization framework which uses the finite element analysis to study how the reinforced concrete industrial chimneys respond to the gravity wind seismic as well as transient gust loads in the ANSYS. The study included the realistic loading conditions which combined the height-dependent wind pressure patterns with the seismic time-history data as well as short burst gust impulses. The researchers used the coupled GA-ANSYS method to optimize the important design parameters which included the wall thickness as well as taper ratio to achieve the better structural performance. The study investigated the modal performance, movement patterns, the stress distribution, base shear forces as well as the dynamic response behavior. The study results showed that the improved vibration control resulted in the smaller displacement as well as base stress reductions. The framework provides engineers with the dependable method to evaluate how the chimney systems function under the intricate dynamic forces present in the real-world engineering situations.

REFERENCES

[1] Sarı, M., Yılmaz, E., & Altunışık, A. C. (2022). Effect of Soil Type on Dynamic Behavior of Reinforced Concrete Industry Chimneys. Recep Tayyip Erdogan University Journal of Science and Engineering, 3(2), 99-114.

[2] Zhou, Y., Chang, M., Wu, H., Zhuo, Y., Djerrad, A., & Lu, X. (2023). Numerical investigation on the characteristics of dynamic response and damage of a RC tall chimney considering vertical ground motions. Soil Dynamics and Earthquake Engineering, 175, 108224.

[3] Krishnan, R., Deshmukh, M. A., Sivakumar, V. L., Joshi, G., Geethakumari, T., & Prakash, F. (2023). Effective tuned mass damper system for RC tall chimney dynamic wind response control. Materials Today: Proceedings.

[4] Allaboudi, E. G., & Ahmida, K. M. Investigation of the dynamic behavior of a chimney at Tripoli-West power plant. Int. Sci. Technol. J, 36(1), 10-62341.

[5] Gupta, A., Choudhary, J., & Sharma, M. (2025). Optimization of RC chimney design under multivariate loads: some insights by Abaqus simulations. Asian Journal of Civil Engineering, 26(8), 3131-3152.

[6] Kumar, S., & Kumar, S. (2022). Wind Load Analysis on High Rise Chimney using Computational Fluid Dynamics. International Research Journal of Engineering and Technology (IRJET), 9(9), 563-566.

[7] Ahmida, K. M., Abuaisha, S. N., Allaboudi, E. G., & Abead, M. S. (2022). Deformation Analysis of a Chimney at Tripoli-West Power Plant. In International Conference on Mechanical and Industrial Engineering ICMIE2022.

[8] Khan, M. M., & Roy, A. K. (2024). Interference effect of buildings on high rise power station chimney subjected to wind: a numerical modelling approach. Innovative Infrastructure Solutions, 9(8), 327.

[9] GS, S., YM, A. K., Pandit, P., & BR, J. (2025). Soil-structure Interaction Effects on Tall Industrial Chimney Subjected to Along-wind Load. Engineering Letters, 33(11).

[10] Khan, M. M., & Roy, A. K. (2024). Numerical investigation of interference effects on tall power station chimney subjecting varying wind incident angles. Journal of Building Pathology and Rehabilitation, 9(2), 122.

[11] Tanriver, K., Etyemez, A., & Ay, M. (2025). Integrated use of finite element analysis and gaussian process regression in the structural analysis of AISI 316 stainless steel chimney systems. Scientific Reports, 15(1), 37858.

[12] Paswan, P., & Mishra, A. (2024, June). Comparative Analysis of Steel Chimney Using Indian Standards (IS) & European Norms (EN). In IOP Conference Series: Earth and Environmental Science (Vol. 1326, No. 1, p. 012024). IOP Publishing.

[13] Fertahi, S. E. D., Rehman, S., Lahrech, K., Samaouali, A., Arbaoui, A., Kadiri, I., & Agounoun, R. (2024). A Review of Comprehensive Guidelines for Computational Fluid Dynamics (CFD) Validation in Solar Chimney Power Plants: Methodology and Manzanares Prototype Case Study. Fluids, 9(11), 251.

[14] Hassan, A. M. (2023). Solar chimney performance driven air ventilation promotion: an investigation of various configuration parameters. Buildings, 13(11), 2796.

[15] Bahar, S., Rijal, A. S., Arrohman, S., Khoeron, S., & Rahmawati, R. (2023, November). SIMULATION ANALYSIS OF THE LOAD EFFECT ON WALKWAY DESIGN FOR CHIMNEY AT PT. X. In The International Conference on Computer Science and Engineering Technology Proceeding (ICCSET) (Vol. 2, No. 1, pp. 9-18).